Simplified diagrammatic expansion for effective operator

Chang-Kui Duan,[1,2] Yun-Gui Gong,[1] Hui-Ning Dong,[1] and Michael F. Reid[2]

[1] *Institute of Applied Physics and College of Electronic Engineering, Chongqing University of Post and Telecommunication, Chongqing 400065, China*

[2] *Department of Physics and Astronomy, University of Canterbury, Christchurch, New Zealand*

(Dated: February 1, 2008)

For a quantum many-body problem, effective Hamiltonians that give exact eigenvalues in reduced model space usually have different expressions, diagrams and evaluation rules from effective transition operators that give exact transition matrix elements between effective eigenvectors in reduced model space. By modifying these diagrams slightly and considering the linked diagrams for all the terms of the same order, we find that the evaluation rules can be made the same for both effective Hamiltonian and effective transition operator diagrams, and in many cases it is possible to combine many diagrams into one modified diagram. We give the rules to evaluate these modified diagrams and show their validity.

I. INTRODUCTION

Effective Hamiltonian $H_{\rm eff}$ and transition operators $O_{\rm eff}$ are commonly used in many *ab initio* many-body calculations[1], such as nuclear, atomic and molecular systems, and in phenomenological calculations[2, 3, 4, 5, 6, 7, 8, 9, 10, 11, 12, 13, 14, 15] of doped transitional metal ions, lanthanide and actinide ions. $H_{\rm eff}$ is defined to be an operator acting on a restricted model space of handleable dimensions to give upon diagonalization the exact eigenvalues and model space eigenvectors. For a time-independent transition operator O, $O_{\rm eff}$ may be introduced that gives the same matrix elements between the model space eigenvectors of $H_{\rm eff}$ as the original operator O between the corresponding true eigenvectors of H. Calculations based on $H_{\rm eff}$ and $O_{\rm eff}$ have many advantages over variational and other direct calculations based on H and O, such as smaller bases, less calculation effort, order by order approximations etc, and can also be used together with variational and other direct calculations[**?**] A recently review can be found in 17.

$H_{\rm eff}$ and $O_{\rm eff}$ are often constructed by time-independent many-body perturbation theory (MBPT) with order-by-order approximation, which can be represented with Goldstone diagrams, in analogy to Feynman diagrams[18]. Many expansions have been given, whose diagrammatic representations usually contain not only connected but also disconnected diagrams, which have the shortcoming of size inconsistency, much more computation efforts and tremendous number of diagrams. Nonetheless, There are common-used effective Hamiltonians, one hermitian and the other nonhermitian are known to contain only connected diagrams.[16] The rules to generate diagrams and to evaluate them are well-known. Factorization theorem is shown to be able to combine diagrams having the same set of vertexes and lines but different relative orderings of vertexes, and hence reduces the number of high-order diagrams.[4] Compared to effective Hamiltonians, effective transition operators generally have different algebraic forms, much more complicated diagrammatic representations, much greater number of diagrams and different diagram evaluation rules. The hermitian (canonical) effective transition operator, which works together with the hermitian (canonical) effective Hamiltonian, has been presented in detail by Hurtubise and co-workers in a series of papers.[1, 9, 16] Duan and Reid[19] constructed a simple connected nonhermitian $O_{\rm eff}$ that works together with the connected nonhermitian effective Hamiltonian and showed how to construct a connected expansion. Since it is well-known that hermitian effective Hamiltonian up to third order can be obtained from trivial symmetrization,[6] and this can also be shown for effective transition operators (up to third order in V, the perturbation in Hamiltonian), and also for higher-order calculations usually coupled-cluster methods come into play, most researches required only limited order diagram calculations of nonhermitian effective Hamiltonian and nonhermitian effective transition operators. However, there are two problems with the effective operator methods: too many diagrams, and the rules to calculate energy denominators for effective transition operators being different from those for effective Hamiltonian.[16]

Our aim in this paper is to modify the diagram representation of many-body perturbation expansion of effective Hamiltonian and effective transition operators, so that the energy denominator rules for effective transition operators and effective Hamiltonian are the same, and the number of diagrams is greatly reduced and becomes handleable for third order terms of nonhermitian effective transition operators. In section II we present our diagrammatic representation of many-body operators and the corresponding evaluation rules for perturbation diagrams; in section III we illustrate the generalized factorization theorem for the effective transition operators; and in Section IV we show how to denote several diagrams of the same set of vertexes and lines with only one diagram to group and reduce the number of diagrams.

II. MODIFIED DIAGRAMS AND THE EVALUATION RULES

We use the following algebraic representation for a general fermion n-body interaction $T_n(1,2,\cdots,n)$:

$$T_n = \frac{1}{n!^2} \sum_{\alpha_1,\cdots,\alpha_n,\beta_1,\cdots,\beta_n} t_{\alpha_1\alpha_2\cdots\alpha_n,\beta_1\beta_2\cdots\beta_n} a^+_{\alpha_1}\cdots a^+_{\alpha_n} a_{\beta_n}\cdots a_{\beta_1}, \quad (1)$$

where the coefficients $t_{\alpha_1\alpha_2\cdots\alpha_n,\beta_1\beta_2\cdots\beta_n}$ are anti-symmetry under exchange of a pair of bra indexes or ket indexes. It can be seen for one and two body interactions, the coefficients are given as follows

$$t_{\alpha,\beta} = \langle\alpha(1)|T_1(1)|\beta(1)\rangle, \quad (2)$$

$$t_{\alpha_1\alpha_2,\beta_1\beta_2} = \langle\alpha_1(1)\alpha_2(2)|T_1(1,2)|\beta_1(1)\beta_2(2)\rangle - \langle\alpha_1(1)\alpha_2(2)|T_1(1,2)|\beta_2(1)\beta_1(2)\rangle, \quad (3)$$

where the indexes in bracket "()" means the indexes of the variables of the function. It is straightforward to give the coefficients for n-body ($n \geq 3$)interactions. The diagrammatic representation of T_n is:

$T_n =$ 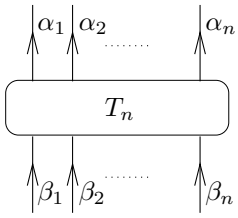

(4)

The diagram is invariant under $n!$ interchange of the n out-going or in-going lines. The number of symmetry operations is $(n!)^2$, which contributes to the factor $1/(n!)^2$ as appeared in Eq. 1. For general close-shell reference "vacuum" state where there are both particle and hole lines, the number of inequivalent diagrams for T_n are $(n+1)^2$, corresponding to the $n+1$ possibilities for the in-going lines (0, 1, $\cdots$, n holes) and out-going lines. Particle line and hole line are inequivalent, and hence the symmetry factor changes accordingly for each diagram.

We need to modify the diagrams slightly so that the evaluation of energy denominators for effective operator is the same as that for non-hermitian Hamiltonian and is simple in general. This simplification helps us using generalized factorization theorem and simplifies diagrams developed in the next two sections. The modifications are shown in Fig.1 and Fig.2.

The general rules for evaluating the diagrams of non hermitian Hamiltonian have been summarized by Brandow[4] and Lindgren and Morrison[18]. The rules of evaluating the diagrams for second order perturbative expansion of effective operator have been given by Hurtubise and Freed [20]. With the new notation (1)-(4), the revised more general diagram evaluation rules can be summarized as follows: 1) draw only one diagram[4]

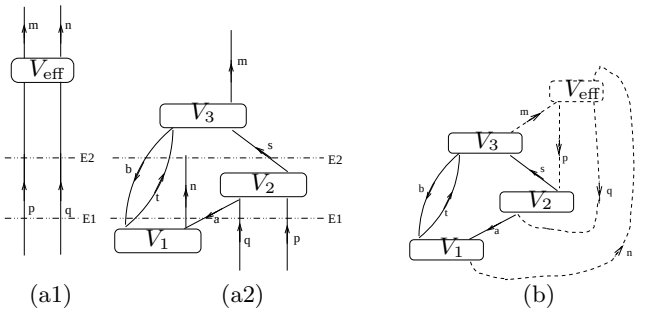

FIG. 1: A two-body third order diagram of non hermitian Hamiltonian, where (a2) is the original diagrams which contributes to the effective interaction showed by diagram (a1), (b) is our modified representation for this diagram, where out-/in- going lines are changed into dashed line and end at dashed interaction vertex $V_{\rm eff}$.

for any one T_n operator; 2) express the evaluation result in the form Eq. (1) and the evaluation becomes calculation of $t_{\alpha_1,\alpha_2,\cdots;\beta_1,\beta_2,\cdots}$ coefficients; 3) in coefficient $t_{\alpha_1,\cdots,\alpha_m;\beta_1,\cdots,\beta_m}$, includes a factor $(m!)^2/(i_1!i_2!\cdots)$, where m ingoing lines and m outgoing lines are participated into sets with i_1, i_2, $\cdots$, equivalent lines, with i lines being equivalent if and only if they all start at the same interaction (or no beginning interaction), and point to the same ending interaction (or no ending interaction); 4) include an over-all sign factor of $(-1)^{l+h}$,[4] where l is the number of closed loops and h the number of downgoing or "hole" line segments; 5) For each vertex, multiple the antisymetrized matrix elements as given in Eq. (3) and (3). 6) for a n-vertex diagram (suppose the vertex are labeled increasing from the bottom as 1, 2, $\cdots$, n), include the products of energy denominators calculated just above the vertex 1, 2, $\cdots$, n, where energy denominators are calculated by energy sum of all down going line taking away the energy sum of all upgoing lines, as show in Fig. 1; 7) sum each upgoing line independently

over all particle states, and each downgoing line independently over all hole states. The exclusion-violating terms which arise from these independent summations must be included.[4]

The energy denominator can be calculated for diagram Fig.1 (a2) as

$$\begin{aligned}
&(E_2(1)-E_2(2))(E_1(1)-E_1(2)) \\
&= [(\epsilon_p+\epsilon_q)-(-\epsilon_a-\epsilon_b+\epsilon_t+\epsilon_n+\epsilon_p+\epsilon_q)][(\epsilon_p+\epsilon_q)-(-\epsilon_b+\epsilon_t+\epsilon_s+\epsilon_n)] \quad (5)\\
&= (\epsilon_a+\epsilon_b-\epsilon_t-\epsilon_n)(\epsilon_b+\epsilon_p+\epsilon_q-\epsilon_t-\epsilon_n-\epsilon_s), \quad (6)
\end{aligned}$$

where $E_i(j)$ is the energy for diagram Fig. 1(ai) calculated at the indicated line by the energies of up-going lines taking away the energies of down-going lines. Diagram Fig. 1 (a2) can be written as

$$\text{Fig. } 1(a2) \;=\; \frac{1}{2!^2}\sum_{mnpq} a_m^+ a_n^+ a_q a_p \left(-(2!)^2/2! \sum_{abts} \frac{(V_c)_{tn,ba}(V_b)_{sa,pq}(V_a)_{mb,st}}{(\epsilon_a+\epsilon_b-\epsilon_t-\epsilon_n)(\epsilon_b+\epsilon_p+\epsilon_q-\epsilon_t-\epsilon_n-\epsilon_s)} \right), \quad (7)$$

where the minus sign comes from the numbers of core solid lines,2, and close cycle,1, adding up to odd number 3. the factor $(2!)^2/2!$ is due to the fact that the effective operator is two-body with equivalent lines p and q.

The calculation of energy denominator can be put in an more systematic way as shown in Fig. 1b: the energy denominator for i^{th} vertex, is just the negative of net outflow energy (E_{noe}) of a loop enclosing vertex 1, 2, $\cdots$, i, i.e.,

$$-E_{\text{noe}}(V_1V_2\cdots V_i) = -(E_{\text{noe}}(V_1)+E_{\text{noe}}(V_2)+\cdots+E_{\text{noe}}(V_i)). \quad (8)$$

Therefore, the energy denominator factor for the $n-$ vertex diagram can be written as

$$\begin{aligned}
D &= (-1)^{n-1}E_{\text{noe}}(V_1)E_{\text{noe}}(V_1V_2)\cdots E_{\text{noe}}(V_1V_2\cdots V_{n-1}) \quad (9)\\
&= (-1)^{n-1}E_{\text{noe}}(V_1)[E_{\text{noe}}(V_1)+E_{\text{noe}}(V_2)]\cdots[E_{\text{noe}}(V_1)+E_{\text{noe}}(V_2)+\cdots E_{\text{noe}}(V_{n-1})]. \quad (10)
\end{aligned}$$

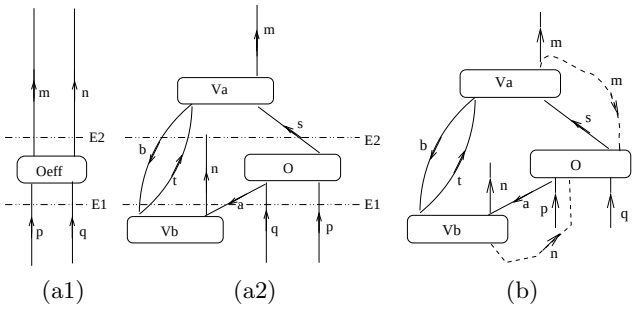

FIG. 2: A second order (in V) diagram of effective transition operator O_{eff}, where V_a and V_b are interactions contained in original Hamiltonian and O is the original transition operator.

For Hermitian effective transition operators and Hamiltonians, the rules to evaluate diagrams have been given by Hurturbise and Freed[20], which is different from Lindgren and Morrison's[18] in energy denominators and contains algebraic factors. When we draw vertex of O_{eff} at the same level as the vertex of O in perturbation diagrams, as shown in Fig. 2(a), the rules of calculating denominators become exactly the same as those for the non-hermitian Hamiltonian. We modify Fig. 2(a) accordingly to give Fig. 2(b). In Fig. 2(b) we save the free lines for the sake of calculating matrix elements. Note that the free lines should not be included in the calculation of denominators and the dashed lines should not be included in the calculation of matrix elements. Diagram Fig. 2(a) can be calculated as

$$\text{Fig. } 2(b) = \frac{1}{4}\sum_{mnpq} a_m^+ a_n^+ a_q a_p \left(-2\sum_{abst} \frac{(V_3)_{mb,st}(V_1)_{nt,ab}O_{as,pq}}{(\epsilon_a+\epsilon_b-\epsilon_t-\epsilon_n)(\epsilon_b+\epsilon_m-\epsilon_t-\epsilon_s)} \right) \quad (11)$$

It can been seen that the rules to calculate the denominators are the same for the two types of diagrams, which are given in Eq. 10.

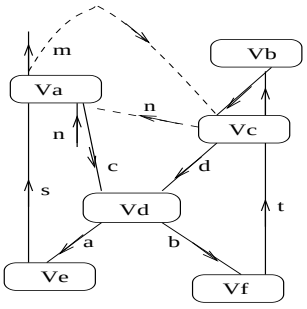

FIG. 3: An example connected diagram with disconnected part at the bottom and on the top to illustrate factorisation theorem.

III. GENERALIZED FACTORIZATION THEOREM FOR THE MODIFIED DIAGRAMS

When several diagrams have the same set of vertexes and the same line directions and line types but different relative orderings of vertexes, they have the same matrix elements, factors and signs but different denominators. If all possible relative orderings are included, the results can be expressed by means of a single diagram with the denominators determined independently for each part of the diagrams[4]. This is the factorization theorem. Lindgren gave a illustration and proof[21]. However it was not trivial to show that this theorem also holds for Hurtubise and Freed's rules of evaluation of denominators for effective interaction diagrams. Here, the rules to evaluate denominators for our modified diagrams are the same for both effective Hamiltonian and effective operator, showing trivially that factorization theorem also holds for effective operator.

A diagram to illustrate this theorem is given in Fig. 3, where V_e and V_f are two disconnected parts at the bottom, and V_a and V_bV_c are two disconnected parts on the top. If one lowers V_e relative to V_f, the vertexes and all the lines (direction and types) do not change, but the denominator from the lowest two interactions change from $E_{\rm noe}(V_f)[E_{\rm noe}(V_e)+E_{\rm noe}(V_f)]$ to $E_{\rm noe}(V_e)[E_{\rm noe}(V_f)+E_{\rm noe}(V_e)]$. By adding those two diagrams together, one gets a denominator $E_{\rm noe}(V_f)E_{\rm noe}(V_e)$, which is the same as calculating the lowest two disconnected interaction separately. The denominator for V_b is $-E_{\rm noe}(V_aV_cV_dV_eV_f)=E_{\rm noe}(V_b)$, which follows from the fact that all $E_{\rm noe}$'s for all vertexes add up to zero. Similarly, the denominator from the highest three interactions is $E_{\rm noe}(V_b)E_{\rm noe}(V_bV_a)E_{\rm noe}(V_bV_aV_c)$ for the ordering showed in Fig. 3. There are two other diagrams with different orderings of V_a relative to V_bV_c. By adding all the three diagrams up, one gets, similar to the case of the lowest two interactions, a denominator from the highest three interactions $E_{\rm noe}(V_a)E_{\rm noe}(V_b)[E_{\rm noe}(V_bV_c)]$. The total denominator calculated this way for the sum of those diagrams with all the possible orderings is $E_{\rm noe}(V_a)E_{\rm noe}(V_b)E_{\rm noe}(V_bV_c)E_{\rm noe}(V_e)E_{\rm noe}(V_f)$. If one uses factorization theorem for both the upper disconnected part and the lower disconnected part, one gets exactly the same denominator much more straightforward. For completeness, we give the result for this diagram as follows:

$$Fig.\ 3 = \sum_{mn} a_m^+ a_n \left((-1)^6 \sum_{abcde,stu} \frac{(V_a)_{mc,sn}(V_b)_{e,u}(V_c)_{ud,te}(V_d)_{ab,cd}(V_e)_{s,a}(V_f)_{tb}}{E_{\rm noe}(V_a)E_{\rm noe}(V_b)E_{\rm noe}(V_bV_c)E_{\rm noe}(V_e)E_{\rm noe}(V_f)} \right) \quad (12)$$

$$= \sum_{mn} a_m^+ a_n \left((-1)^8 \sum_{abcde,stu} \frac{(V_a)_{mc,ns}(V_b)_{e,u}(V_c)_{ud,et}(V_d)_{ab,cd}(V_e)_{s,a}(V_f)_{tb}}{E_{\rm noe}(V_a)E_{\rm noe}(V_b)E_{\rm noe}(V_bV_c)E_{\rm noe}(V_e)E_{\rm noe}(V_f)} \right). \quad (13)$$

$$= \sum_{mn} a_m^+ a_n \left(\sum_{abcde,stu} \frac{(V_a)_{mc,ns}(V_b)_{e,u}(V_c)_{ud,et}(V_d)_{ab,cd}(V_e)_{s,a}(V_f)_{tb}}{(\epsilon_c+\epsilon_m-\epsilon_n-\epsilon_s)(\epsilon_e-\epsilon_u)(\epsilon_n+\epsilon_d-\epsilon_t-\epsilon_m)(\epsilon_e-\epsilon_s)(\epsilon_b-\epsilon_t)} \right). \quad (14)$$

The sign $(-1)^6$ comes from the fact that there are five backwards solid internal lines and one loop ($edbtue$). If one switches the entering points of s and n at vertex V_a, and e and t at vertex V_c, then one gets the equivalent diagram with three loops. The result for this diagram is given in (13).

IV. DIAGRAMS WITH THE SAME SET OF VERTEXES AND LINE DIRECTIONS AND NOTATIONS

The diagrams in Fig. 4. (b), (c), (d) and (e) have the same set of vertexes, line connections and directions. One can simply denote the four diagrams as diagram (a), where i and j can be both core lines and virtual lines. Hence the matrix elements, the symmetry factors and the $E_{\rm noe}$'s have the same form. The denominators are

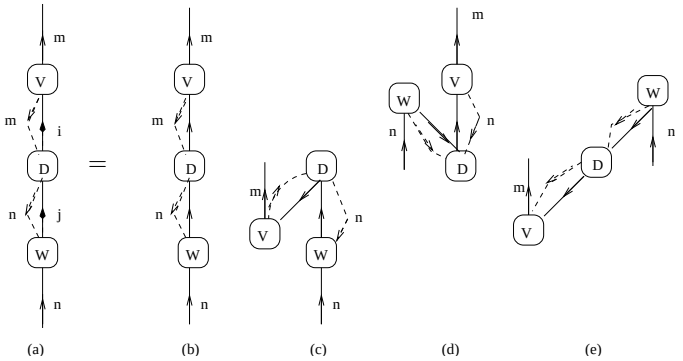

FIG. 4: An example to demonstrate the combination of several diagrams with the same set of vertexes, line connections and directions into one diagram. Here (b) has two particle-state internal lines, (c) and (d) each has one hole-state internal line and one particle-state internal line, (e) has two hole-state internal lines, and (a) is a diagram used to denote all the four diagrams (b) to (e).

just different combinations of $E_{\rm noe}$'s. One cannot combine the denominators together the same way as in the factorisation theorem since the orbital types for different diagrams are different. However, this does not prevent us from using (a) to represent all the four diagrams as long as one is cautious about the relations between the relative orderings of vertexes and the internal line types in evaluating diagram (a).

$$\begin{aligned} \text{Fig. 4} &= \sum_{mn} a_m^+ a_n \left(\sum_{i,j} \eta_1(i,j) \frac{V_{mi} D_{ij} V_{jn}}{\eta_2(i,j) E_{\rm noe}(V) E_{\rm noe}(W)} \right) \\ &= \sum_{mn} a_m^+ a_n \left(\sum_{i,j} \frac{V_{mi} D_{ij} V_{jn}}{(\epsilon_n - \epsilon_j)(\epsilon_m - \epsilon_i)} \right), \end{aligned} \tag{15}$$

where $\eta_1(i,j) = 1, -1, -1, 1$ and $\eta_2(i,j) = -1, 1, 1, -1$ are the sign contributed by core orbitals and denominators respectively. Note that factorisation theorem has been applied in the evaluation of diagrams (c) and (d).

Denote the line entering V_1 and then passing sequentially $V_2, \cdots, V_{n-1}$ and finally going out from V_n as $(V_n V_{n-1} \cdots V_2 V_1)$, the loop passing sequential $V_1, V_2, \cdots, V_n, V_1$ and pointing from V_1 to V_2 as $(V_1 V_n \cdots V_2 V_1)$, and the ordering that A is higher then B as $[AB]$. It can be seen that diagram Fig. 4a is uniquely specified by (VDW) and diagram Fig. 4b-e are $(VDW)[VDW]$,$(VDW)[DVW + DWV]$,$(VDW)[VWD+WVD]$ and $(VDW)[WDV]$. As has been argued above, one only needs to draw one diagram to work out the values of all those similar diagrams by using the denominator rule Eq. 10 and other standard rules for matrix elements and factors. The application of these new notations to one and two-photon transitions can greatly reduce the number of diagrams. This will be presented elsewhere latter.

V. CONCLUSION

We have modified the diagrams for non-hermitian effective Hamiltonians and effective operators so that the rules to calculate the denominators are the same for the two types of diagrams. Expressed with these modified diagrams, proof of factorization theorem for effective transition operators becomes trivial. By denoting the class of diagrams of the same set of vertexes, line connections and directions with one diagram, the number of diagrams can be greatly reduced and hence making the high order contributions to effective operators more handleable.

[1] V. Hurtubise and K. F. Freed, Adv. Chem. Phys. **83**, 405 (1993).
[2] I. Lindgren, Rep. Prog. Phys. **47**, 345 (1984).
[3] J. J. Oleksik and K. Freed, J. Chem. Phys. **79**, 1396 (1983).
[4] B. H. Brandow, Rev. Mod. Phys. **39**, 771 (1967).
[5] P. J. Ellis and E. Osnes, Rev. Mod. Phys. **49**, 777 (1977).
[6] Brandow, *in Effective Interactions and Operators in Nuclei, edited by B. R. Barrett* (Springer-Verlag, Berlin, 1975).
[7] B. H. Brandow, Adv. Quantum Chem. **10**, 187 (1977).
[8] F. Jϕrgensen and T. Pedersen, Mol. Phys. **27**, 33 (1974).
[9] K. F. Freed, *in Many-Body Methods in Quantum Chemistry, edited by U. Kaldor* (Springer-Verlag, Berlin, 1989).
[10] X. C. Wang and K. F. Freed, J. Chem. Phys. **91**, 1142 (1989).
[11] X. C. Wang and K. F. Freed, J. Chem. Phys. **94**, 5253 (1991).
[12] X. C. Wang and K. F. Freed, J. Chem. Phys. **91**, 3002 (1989).
[13] A. W. Kanzler and K. F. Freed, J. Chem. Phys. **94**, 3778 (1991).
[14] C. Duan, M. Reid, and G. Burdick, Phys. Rev. B **66**, 155108 (2002).
[15] D. Aberg, S. Edvardsson, and M. Engholm, Phys. Rev. B **68**, 195105 (2003).
[16] V. Hurtubise, J. Chem. Phys. **99**, 265 (1993).
[17] J. P. Killingbeck and G. Jolicard, J. Phys. A: Math. Gen.**36**, R105 (2003).
[18] I. Lindgren and J. Morrison, *Atomic Many-Body Theory (2nd edition), Springer Series on Atoms and Plasmas, Vol.3* (Springer-Verlag, New York, 1985).
[19] C. Duan and M. F. Reid, J. Chem. Phys **115**, 8279 (2001).
[20] V. Hurtubise and K. F. Freed, J. Chem. Phys **100**, 4955 (1994).
[21] I. Lindgren, Phys. Scr. **32**, 611 (1974).